*Cerebral Cortex*, August 2016;26: 3494–3507

**doi:10.1093/cercor/bhw134**
Advance Access Publication Date: 18 May 2016
Original Article

ORIGINAL ARTICLE

# Motor Training Promotes Both Synaptic and Intrinsic Plasticity of Layer II/III Pyramidal Neurons in the Primary Motor Cortex

Hiroyuki Kida[1], Yasumasa Tsuda[1], Nana Ito[1], Yui Yamamoto[2], Yuji Owada[2], Yoshinori Kamiya[3], and Dai Mitsushima[1]

[1]Department of Physiology, [2]Department of Organ Anatomy, Yamaguchi University Graduate School of Medicine, 1-1-1 Minami-Kogushi, Ube, Yamaguchi 755-8505, Japan and [3]Uonuma Institute of Community Medicine, Niigata University Medical and Dental Hospital, 4132 Urasa, Minami-uonuma, Niigata 949-7302, Japan

Address correspondence to Dai Mitsushima, Department of Physiology, Yamaguchi University Graduate School of Medicine, 1-1-1 Minami-Kogushi, Ube, 755-8505, Japan. Email: mitsu@yamaguchi-u.ac.jp

## Abstract

Motor skill training induces structural plasticity at dendritic spines in the primary motor cortex (M1). To further analyze both synaptic and intrinsic plasticity in the layer II/III area of M1, we subjected rats to a rotor rod test and then prepared acute brain slices. Motor skill consistently improved within 2 days of training. Voltage clamp analysis showed significantly higher α-amino-3-hydroxy-5-methyl-4-isoxazolepropionic acid/*N*-methyl-D-aspartate (AMPA/NMDA) ratios and miniature EPSC amplitudes in 1-day trained rats compared with untrained rats, suggesting increased postsynaptic AMPA receptors in the early phase of motor learning. Compared with untrained controls, 2-days trained rats showed significantly higher miniature EPSC amplitude and frequency. Paired-pulse analysis further demonstrated lower rates in 2-days trained rats, suggesting increased presynaptic glutamate release during the late phase of learning. One-day trained rats showed decreased miniature IPSC frequency and increased paired-pulse analysis of evoked IPSC, suggesting a transient decrease in presynaptic γ-aminobutyric acid (GABA) release. Moreover, current clamp analysis revealed lower resting membrane potential, higher spike threshold, and deeper afterhyperpolarization in 1-day trained rats—while 2-days trained rats showed higher membrane potential, suggesting dynamic changes in intrinsic properties. Our present results indicate dynamic changes in glutamatergic, GABAergic, and intrinsic plasticity in M1 layer II/III neurons after the motor training.

**Key words:** AMPA receptor, GABA, glutamic acid, motor learning

## Introduction

The primary motor cortex (M1) is considered a central region required for skilled voluntary movements. During voluntary movements, neurons of the M1 vigorously discharge to encode various parameters, such as force (Evarts 1968), direction (Georgopoulos et al. 1982), and speed of spontaneous movements (Moran and Schwartz 1999). M1 neurons form a glutamatergic/γ-aminobutyric acidergic (GABAergic) neural circuit (Kaneko 2013), and synaptic transmission efficacy can be altered through motor experience. For example, forelimb motor training reportedly strengthens horizontal connections in M1 layer II/III (Rioult-Pedotti et al. 1998, 2000). In vivo imaging studies further demonstrated structural remodeling of dendritic spines of the M1 pyramidal neurons after skilled motor tasks, suggesting the learning-dependent

plasticity of the M1 (Xu et al. 2009; Yang et al. 2009; Yu and Zuo 2011; Ma et al. 2016).

Dendritic spines express glutamate receptors on their postsynaptic surface (Shi et al. 1999; Takumi et al. 1999). Activation of α-amino-3-hydroxy-5-methyl-4-isoxazolepropionic acid (AMPA)-type glutamate receptors induces fast excitatory transmission enabling memory and enhancement of task-related behavior, and *N*-methyl-D-aspartate (NMDA) receptor activation is implicated in maintenance of spatial memory and associative learning (Riedel et al. 2003). Studies using virus-mediated in vivo gene delivery with in vitro patch-clamp recordings have also demonstrated that AMPA receptor delivery into the synapses is involved in synaptic strengthening (Malinow and Malenka 2002; Takahashi et al. 2003). Recently, we further showed that AMPA receptor delivery into CA1 synapses is required for episodic memory (Mitsushima et al. 2011). Since the LTP-like plasticity of M1 contributes to motor skill retention (Rioult-Pedotti et al. 2000; Cantarero et al. 2013), we hypothesized that an increase of postsynaptic AMPA receptors leads to synaptic strengthening among layer II/III neurons.

Most research regarding plasticity focuses on excitatory synapses, but GABAergic inhibitory synapses are also strengthened by frequent presynaptic fiber stimulation (Caillard et al. 1999; Kurotani et al. 2008). Experience-dependent plasticity of GABAergic synapses was first reported in the hippocampus (Cui et al. 2008). We further demonstrated that contextual memory requires both AMPA and $GABA_A$ receptor-mediated postsynaptic plasticity, forming a wide diversity of excitatory/inhibitory inputs at hippocampal CA1 synapses (Mitsushima et al. 2013). However, motor learning rapidly reduces local GABA concentration in the human sensorimotor cortex (Floyer-Lea et al. 2006), suggesting that skilled motor learning may reduce GABAergic inhibitory transmission in the M1. In the present study, we further examined motor training-dependent plasticity at GABAergic synapses, as well as the balance of excitatory/inhibitory synaptic inputs (Liu 2004).

Neuronal excitability after learning is impacted by synaptic plasticity, but also by long-term changes in neuronal properties, such as membrane potential, spike threshold, and afterhyperpolarization (Daoudal and Debanne 2003; Saar and Barkai 2003). In the hippocampus, operant conditioning training changes the intrinsic properties of CA1 neurons, without affecting the resting membrane potential or resistance (Moyer et al. 1996; Saar et al. 1998). Olfactory training reduces afterhyperpolarization to enhance excitability in the piriform cortex, suggesting long-term plasticity of intrinsic excitability (Saar and Barkai 2003). However, it is completely unknown whether motor training changes neuronal properties in the M1.

Here we show that an accelerated rotor rod task promoted dynamic changes in the glutamatergic, GABAergic, and intrinsic plasticity in M1 layer II/III neurons. These findings provide functional evidence for the structural remodeling of dendritic spines after the motor skills training.

## Materials and Methods

### Animals

Male Sprague-Dawley rats ($n = 166$, Chiyoda Kaihatsu Co., Tokyo, Japan) were housed in individual plastic cages (40 × 25 × 25 cm), maintained at a constant temperature of 23 ± 1°C under a 12-h light/dark cycle, with water and food provided ad libitum. We used 67 rats for electrophysiology, 48 rats for Western blotting, and 51 rats for microinjection studies. All experiments were performed according to the Guidelines for Animal Experimentation of Yamaguchi University School of Medicine, and approved by the Institutional Animal Care and Use Committee of Yamaguchi University.

### Motor Learning Test

To evaluate changes in motor skills, we conducted the rotor rod test (ENV577; Med Associates Inc., St. Albans, VT, USA) with 4-week-old rats (Fig. 1*A*). Rats were assigned to either the naive group (untrained), the training group for one day (1-day trained), or the training group for 2 successive days (2-days trained). For each test, the rats were allowed 10 attempts with a 30-s time interval between trials. But in Figure 1*D*, the rats were subjected additional 5 attempts after the bilateral microinjections of drugs. The interval between the 10th trial and the 11th trial was 1–2 min. The rotor rod was set to increase from 4 to 40 rpm over 5 min, and the duration of rod-riding was recorded.

### Microinjection of Drugs

To investigate how glutamatergic neurotransmission impacted motor function, CNQX or APV was infused into M1 layers II/III. With the rats under sodium pentobarbital anesthesia (30–50 mg/kg, i.p.), a stainless-steel guide cannula (CXGW-4; Eicom Co., Kyoto, Japan) was bilaterally implanted into the M1 layer II/III region according to the brain atlas (Paxinos and Watson 1998). The coordinates were 1.2 mm anterior to bregma, 2.0 mm lateral to the midline, and 0.3 mm below the dura surface. After cannula implantation, a stylet was inserted into the guide until drug injection (Mitsushima et al. 2009, 2013).

One to 3 days after cannula implantation, the stylet was replaced with an injector and the experiment was conducted. We performed bilateral microinjection of vehicle (1 µL 13% DMSO per side), CNQX (1 µg/µL per side), or APV (1 µg/µL per side). Total amount of microinjection was 2 µL/animal. One minute following completion of injections, the injector cannula was removed from the guides. To investigate the mechanism of memory acquisition, the first trial on the first day of training was initiated immediately after bilateral microinjection of vehicle, CNQX, or APV into the M1.

To confirm acute effect of bilateral microinjection of CNQX on motor function, 1-day trained rats were tested in an open field test for 5 min immediately after the bilateral microinjection of vehicle or CNQX. The open field was a rectangular plastic box (length: 50 cm, width: 50 cm, height: 40 cm) with its floor equally divided into 36 squares and illuminated by white light (20 W). Sixteen squares were defined as the center, remaining 20 squares as the periphery. A rat was placed the center of the apparatus and its exploration was recorded with a video camera connected to tracer software (Muromachi Kikai Co., Tokyo, Japan). After the video recording, we analyzed time spent in the center area and total traveled distance during 5 min.

### Electrophysiology

Thirty minutes after their final rotor rod test, the 1-day or 2-days trained rats were anesthetized with pentobarbital, acute brain slices were prepared and whole-cell recordings were performed as previously described (Mitsushima et al. 2011, 2013). Briefly, the brains were quickly perfused with ice-cold dissection buffer (25.0 mM $NaHCO_3$, 1.25 mM $NaH_2PO_4$, 2.5 mM KCl, 0.5 mM $CaCl_2$, 7.0 mM $MgCl_2$, 25.0 mM glucose, 110.0 mM choline chloride, and 11.6 mM ascorbic acid) and gassed with 5% $CO_2$/95% $O_2$. Coronal brain slices were cut into 350-µm slices with a Leica

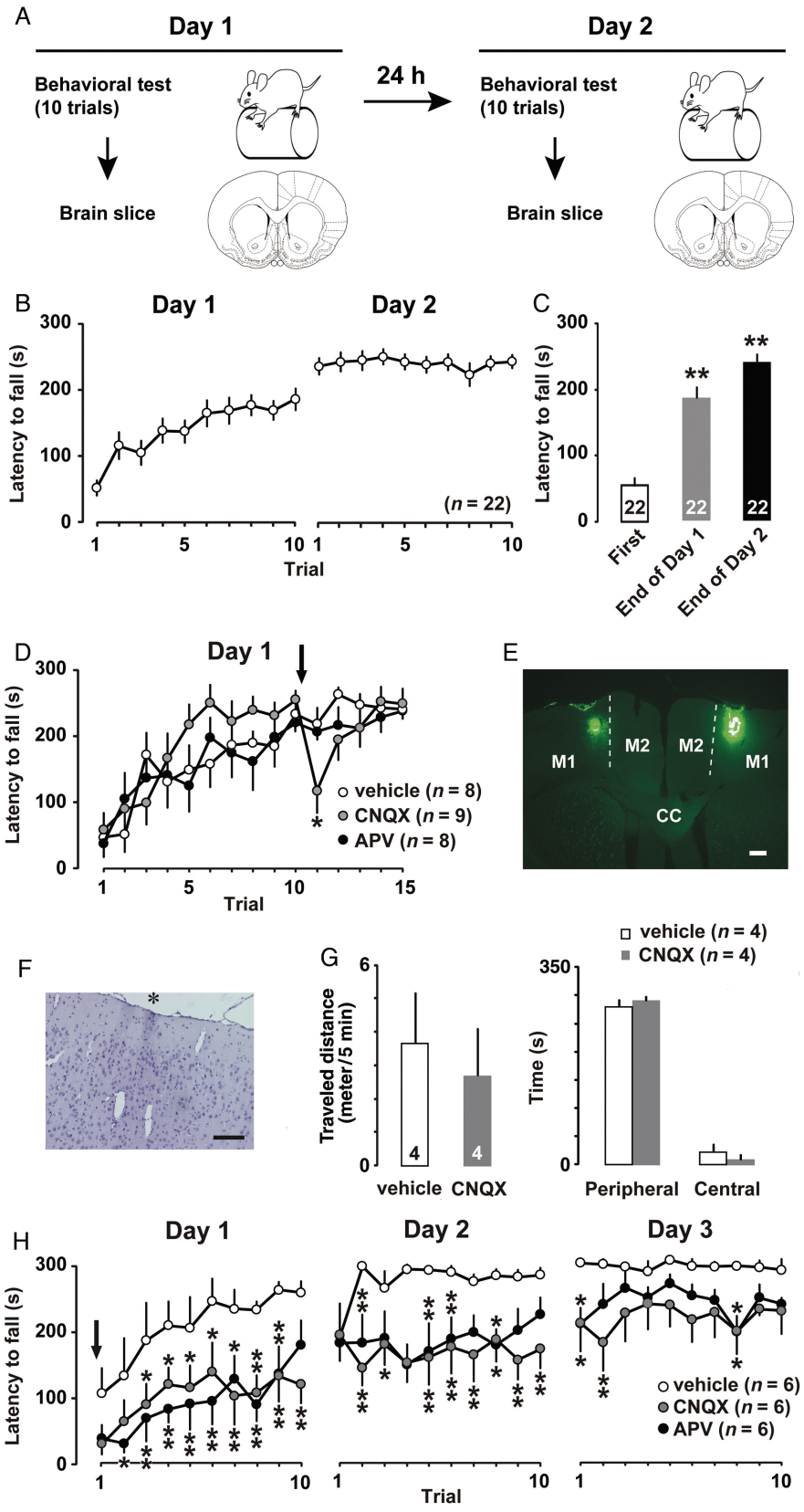


**Figure 1.** (*A*) Experimental design of the rotor rod task. (*B*) Mean latency to fall from the barrel plotted for each trial (10 trials/day) in 2-days trained rats. (*C*) Mean latency at the first trial and the final trial on the first and second days of training. $^{**}P < 0.01$ versus first. (*D*) Vehicle (open), CNQX (gray), or APV (filled) was bilaterally injected into the M1 after the 10th trial. $^{*}P < 0.05$ versus vehicle. (*E*) Visualization of the microinjected site in the M1. CC, corpus callosum; M2, secondary motor cortex. (*F*) Hematoxylin staining of injection site (black asterisk). Scale bars, 200 μm. (*G*) Open field performance immediately after the bilateral microinjection of CNQX. (*H*) Vehicle, CNQX, or APV was bilaterally microinjected into the M1 before the 1st trial. Arrows indicate the microinjection timing. The number of rats in each group is shown in parentheses or at the bottom of each bar. $^{*}P < 0.05$, $^{**}P < 0.01$ versus vehicle. Error bars indicate ± SEM .

vibratome (VT-1200; Leica Biosystems, Nussloch, Germany) in dissection buffer and transferred to physiological solution (22–25°C, 118 mM NaCl, 2.5 mM KCl, 26 mM $NaHCO_3$, 1 mM $NaH_2PO_4$, 10 mM glucose, 4 mM $MgCl_2$, and 4 mM $CaCl_2$, pH 7.4, gassed with 5% $CO_2$/95% $O_2$). We maintained 3–4 slices from each rat, and then selected 1–2 brain slices for patch recordings based on the brain atlas by Paxinos and Watson (1998). Glass electrodes were made with a horizontal puller (Model P97; Sutter Instrument, Novato, CA, USA) and filled with a suitable solution. Whole-cell recordings were obtained from pyramidal neurons of M1 layer II/III, using an Axopatch-1D amplifier (Axon Instruments Inc., Union City, CA, USA). Recordings were digitized using a Digidata 1440 AD board (Axon), recorded at 5 kHz, and analyzed offline with pCLAMP 10 software (Axon).

The coordinates of recording cells were ~1.2 mm anterior to bregma, 2.0 mm lateral to the midline, and 0.2–0.3 mm below the dura surface: the region corresponding to M1 forelimb representation (Neafsey et al. 1986; Kleim et al. 2002).

### Voltage Clamp Recordings

The recording chamber was perfused with 22–25°C physiological solution. For the analysis of AMPA/NMDA ratio, we added 0.1 mM picrotoxin to block $GABA_A$ receptor-mediated inhibition, and 4 μM 2-chloroadenosine to stabilize evoked neuronal responses (Baidan et al. 1995). Patch recording pipettes (4–7 MΩ) were filled with intracellular solution (115 mM cesium methanesulfonate, 20 mM CsCl, 10 mM HEPES, 2.5 mM $MgCl_2$, 4 mM $Na_2ATP$, 0.4 mM $Na_3GTP$, 10 mM sodium phosphocreatine, and 0.6 mM EGTA at pH 7.25). A bipolar tungsten stimulating electrode (Unique Medical Co., Ltd., Tokyo, Japan) was positioned in the M1 region at 200–300 μm lateral from the recorded neurons. Stimulus intensity was increased from 0.4 to 0.7 mA until a synaptic response with amplitude of >10 pA was recorded. The AMPA/NMDA ratio was calculated as the ratio of the peak current at −60 mV to the current at + 40 mV at 150 ms after stimulus onset (50–100 traces were averaged for each holding potential).

### Miniature Recordings

For miniature recordings, we used modified intracellular solution to adjust the reversal potential of the $GABA_A$ receptor response (127.5 mM cesium methanesulfonate, 7.5 mM CsCl, 10 mM HEPES, 2.5 mM $MgCl_2$, 4 mM $Na_2ATP$, 0.4 mM $Na_3GTP$, 10 mM sodium phosphocreatine, 0.6 mM EGTA, pH 7.25). Moreover, we added 0.5 μM tetrodotoxin (TTX; Wako Pure Chemical Industries Ltd., Osaka, Japan) and 0.1 mM APV (Sigma-Aldrich Co., Tokyo, Japan) to perfusate to block both action potentials and NMDA receptor-mediated excitatory postsynaptic currents. The voltage was clamped at −60 mV for mEPSC recording, and at +15 mV for mIPSC recording. We analyzed the frequency and amplitude of mEPSCs/mIPSCs above 10 pA. To calculate excitation and inhibition (E/I) balance, the value of miniature excitatory postsynaptic current (mEPSC) frequency or amplitude was divided by corresponding value of miniature inhibitory postsynaptic current (mIPSC) frequency or amplitude in each neuron. After recording, we confirmed that mEPSCs and mIPSCs were completely abolished by 10 μM CNQX (Sigma) and 10 μM bicuculline methiodide (Sigma), respectively.

### Paired-Pulse Stimulation

To analyze presynaptic plasticity at excitatory synapses, we added 0.1 mM picrotoxin and 4 μM 2-chloroadenosine to the perfusate and performed paired-pulse stimulation at −60 mV. To analyze presynaptic plasticity at inhibitory synapses, we added 0.1 mM APV and 4 μM 2-chloroadenosine to the perfusate and performed paired-pulse stimulation at +15 mV. To evaluate the paired-pulse ratio from the EPSC or IPSC average, 50–100 sweeps were recorded with paired stimuli at 100-ms intervals. The ratio of the second amplitude to the first amplitude was calculated as the paired-pulse ratio.

### Current Clamp Recordings

For current clamp recordings, pipettes were filled with 130 mM K-Gluconate, 5 mM KCl, 10 mM HEPES, 2.5 mM $MgCl_2$, 4 mM $Na_2ATP$, 0.4 mM $Na_3GTP$, 10 mM Na-phosphocreatine, and 0.6 mM EGTA at pH 7.25. Liquid junction potential was not corrected. During 300-ms current injections from −100 to +400 pA, we counted the numbers of spikes in neurons. To determine the threshold for each neuron, we identified the minimal voltage for action potential induction. The amplitude of afterhyperpolarization was evaluated by measuring the voltage at spike initiation and the lowest voltage during AHP (van der Velden et al. 2012).

To further examine the role of AMPA and NMDA receptors on changes of intrinsic properties, CNQX (1 μg/μL) or APV (1 μg/μL) was unilaterally microinjected into the M1 prior to the motor training. After the 10 sessions of training on day 1, we made acute brain slices of drug-injected side for the current clamp analyses (Fig. 7)

### Western Blotting

Western blotting was performed according to the previous study (Yamamoto et al. 2013). Thirty minutes after training, the brain was removed and incubated for 3 min in ice-cold buffer containing 0.32 M sucrose and 20 mM Tris–HCl (pH 7.5). Dissected motor cortical tissues were homogenized in 200 μL of buffer containing 50 mM Tris–HCl (pH 7.4), 0.5% Triton X-100, 0.5 M NaCl, 10 mM EDTA, 4 mM EGTA, 1 mM $Na_3VO_4$, 50 mM NaF, 40 mM sodium pyrophosphate, 1 mM protease inhibitor, and 1 mM DTT. Insoluble material was removed by a 10-min centrifugation at 15,000 rpm.

For the analysis of synaptosomal fraction, we used the Syn-PER Reagent (Thermo Scientific) with protease/phosphatase inhibitor cocktail (100×). Briefly, samples were centrifuged at 1200 G for 10 min, and the remaining supernatant centrifuged at 15 000 G for 20 min to obtain synaptosome pellet. The resulting pellet was resuspended in 50 μL of lysis buffer. Samples containing equivalent amounts of protein based on the bicinchoninic acid analysis (Thermo Scientific, Rockford, IL, USA) were heated at 100°C for 3 min in Laemmli sample buffer and subjected to SDS-PAGE for 30 min at 200 V. Proteins were transferred to an Immobilon PVDF membrane for 1 h at 100 V. Membranes were blocked for 1 h at room temperature in T-TBS solution containing 50 mM Tris–HCl (pH 7.5), 150 mM NaCl, 0.1% Tween 20, and 5% skim milk, followed by overnight incubation at 4°C with anti-GluA1 (1:1000; Millipore, Tokyo, Japan), anti-phospho-GluA1 ($Ser^{831}$) (1:1000; Millipore), and anti-β-Tubulin (1:1000; BioLegend, San Diego, CA, USA). This step was followed by incubation with HRP-conjugated goat anti-rabbit IgG for phospho-GluA1 (1:5000, Millipore) and HRP-conjugated goat anti-mouse IgG (1:5000, Millipore) for GluA1 and β-Tubulin.

Bound antibodies were visualized using an enhanced chemiluminescence detection system (GE Healthcare, Chalfont St. Giles, UK) and semiquantitatively analyzed using the Image-J program (National Institutes of Health, Bethesda, MD, USA).

### Histology

To confirm the injected sites, we further microinjected a retrograde tracer after the behavioral experiment (Fig. 1E, LumaFluor

Inc., Durham, NC, USA). The animals were deeply anesthetized and perfused with a 4% paraformaldehyde solution. Frozen coronal sections (50-μm thick) were sequentially cut using a microtome. The location of the microinjected site was microscopically verified in the frozen sections.

Some rats were used for hematoxylin staining without the tracer microinjection (Fig. 1F). The animals were deeply anesthetized and perfused transcardially with phosphate-buffered saline, followed by 4% paraformaldehyde in phosphate buffer. The brain was removed and post-fixed in 4% paraformaldehyde for 4–12 h. The brain was embedded in paraffin, and then cut into coronal sections (4-μm thick) with the microtome. Sections were affixed to silane-coated glass slides for staining.

### Data Analysis

To determine the development of motor skill, the data on the latency to fall were analyzed by one-way analysis of variance (ANOVA) with repeated-measures followed by post hoc analysis with the Fisher's protected least significant difference (PLSD) test, where variable was trial. To compare the latency to fall between the drug-injected groups, we used 2-way ANOVA with repeated-measures, followed by post hoc ANOVAs with the Fisher's PLSD test. To compare the differences between 2 groups in open field study, we used unpaired 2-tailed *t*-test.

To compare the means of multiple individual groups, we used one-way factorial ANOVA followed by post hoc analysis with Fisher's PLSD test. E/I balance was analyzed using the Kruskal–Wallis test followed by post hoc analysis with Scheffe's test. To evaluate correlations between mEPSC and mIPSC parameters, we calculated Spearman's correlation coefficient. The current injection data were analyzed by 2-way ANOVA with repeated measures followed by post hoc ANOVAs with the Fisher's PLSD test. *P* values of <0.05 were considered statistically significant.

## Results

Rats were subjected to the rotor rod test (Fig. 1A). Figure 1B shows the average latency to falling from the rotating rod, with longer latency considered to indicate better motor performance. On the first training day, rats clearly improved their motor performance from their first to last trial. On the second training day, their performance reached nearly asymptotic levels, indicating that 2 days of training was sufficient for them to acquire the motor skill. One-way repeated-measures ANOVA found the main effect of trial ($F_{(19,439)} = 17.224$; $P < 0.001$). Briefly, the average latency was 54.8 ± 11.9 s at the first trial, 189.5 ± 17.0 s at the final trial on the first day and 243.5 ± 10.7 s at the final trial on the second day, respectively (Fig. 1C). Compared with the latency at first trial, post hoc analysis further showed significant improvements at final trials on the first ($P < 0.01$) and second training days ($P < 0.01$).

To examine the role of glutamatergic transmission on behavioral performance, we bilaterally microinjected the AMPA receptor antagonist CNQX (1 μg/μL), the NMDA receptor antagonist APV (1 μg/μL), or vehicle (13% DMSO, 1 μL) into M1 layer II/III immediately after the 10th rotor rod trial (Fig. 1D). In this study, 2-way repeated-measures ANOVA found the main effect of trial ($F_{(14,330)} = 11.44$; $P < 0.001$). However, neither the main effects of drug ($F_{(2,330)} = 1.268$; $P = 0.28$) nor the interaction ($F_{(28,\ 330)} = 1.155$; $P = 0.27$) were significant, since the data of Figure 1D contains many points before the drug injection.

Motor performance was transiently impaired following bilateral microinjection of CNQX, but not vehicle or APV, suggesting a role of AMPA receptors on skilled motor performance ($F_{(2,15)} = 3.08$; $P = 0.046$, one-way factorial ANOVA). We confirmed microinjected sites by the retrograde tracer (Fig. 1E) and hematoxylin staining (Fig. 1F). Guide cannula implantation and drug microinjection induced neither gliosis nor intracranial hemorrhage.

CNQX may induce a transient motor deficit in 1-day trained rats. To confirm the possible deficit, we bilaterally microinjected CNQX immediately after the 10th trial in the 1-day trained rats, and then checked open field performances instead of additional rotor rod test (Fig. 1G). The microinjections of CNQX affect neither traveled distance ($t = 0.48$, $P = 0.65$, unpaired *t*-test) nor the duration in the areas ($t = 0.75$, $P = 0.48$, unpaired *t*-test).

We also performed bilateral microinjection of CNQX, APV, or vehicle prior to the first training (Fig. 1H). Two-way repeated-measures ANOVA found the main effects of drug ($F_{(2,450)} = 91.97$; $P < 0.001$) and trial ($F_{(29,450)} = 9.45$; $P < 0.001$), but the interaction was not significant ($F_{(58,450)} = 0.61$; $P = 0.99$). Compared with vehicle injected controls, post hoc ANOVA showed significant impairment of motor performance after the bilateral pretreatment with CNQX ($F_{(1,300)} = 147.49$; $P < 0.001$) or APV ($F_{(1,300)} = 148.17$; $P < 0.001$). Further post hoc comparison at each trial was shown in Figure 1H.

To investigate motor training-dependent plasticity at the synapse level, we prepared acute brain slices for voltage clamp analyses (Fig. 2A). We electrically stimulated horizontal connections to evoke EPSC in layer II/III neurons, and analyzed AMPA receptor-mediated currents at −60 mV and NMDA receptor-mediated currents at +40 mV. The AMPA/NMDA ratio was 309.5 ± 31.4% in untrained, 458.2 ± 36.6% in 1-day trained, and 353.8 ± 30.6% in 2-days trained rats. One-way factorial ANOVA followed by post hoc analysis showed a significant increase in AMPA/NMDA ratio in 1-day trained rats compared with that in untrained rats (Fig. 2B and C; $F_{(2,148)} = 4.96$; $P = 0.008$). We did not observe a high ratio in 2-days trained rats, probably due to the increased NMDA currents (Watt et al. 2004).

Phosphorylation of the AMPA receptor GluA1 subunit at $Ser^{831}$ seems to be required for receptor trafficking into the postsynaptic membrane to induce hippocampal LTP (Lee et al. 2003; Whitlock et al. 2006). To analyze the phosphorylation using Western blot, we trimmed M1 tissue containing surface layers (layers I–III, Fig. 3). Although GluA1 protein levels in the whole-cell fractions were not changed on test days (Fig. 3B; untrained, 100.0 ± 8.8%, 1-day trained, 92.6 ± 12.2%, 2-days trained, 84.6 ± 21.7%; $F_{(2,21)} = 0.30$; $P = 0.75$, one-way factorial ANOVA), $Ser^{831}$ phosphorylation of the GluA1 subunit was significantly increased at 30 min after motor training in both 1-day and 2-days trained rats (Fig. 3C; untrained, 100.0 ± 8.2%, 1-day trained, 140.6 ± 14.3%, 2-days trained, 137.9 ± 13.3%; $F_{(2,21)} = 3.15$; $P = 0.044$, one-way factorial ANOVA).

We further assessed the $Ser^{831}$ phosphorylation in the synaptosomal fraction of the trimmed cortical tissue (Fig. 3D). Although the 1-day trained rats exhibited a significant increase in GluA1 subunit (Fig. 3E; untrained, 100.0 ± 7.8%, 1-day trained, 147.5 ± 3.7%, 2-days trained, 83.7 ± 7.6%; $F_{(2,21)} = 22.4$; $P < 0.001$, one-way factorial ANOVA), normalized levels of $Ser^{831}$ phosphorylation were not changed (Fig. 3F; untrained, 100.0 ± 7.5%, 1-day trained, 86.3 ± 7.5%, 2-days trained, 100.9 ± 11.6%; $F_{(2,21)} = 0.76$; $P = 0.48$, one-way factorial ANOVA). By analyzing the PSD95 expression, we confirmed the validity of the fraction.

We recorded miniature EPSCs (mEPSCs) in the presence of 0.5 μM TTX (Fig. 4A) at −60 mV. One-day trained rats exhibited a significant increase only in mEPSC amplitude, while 2-days trained rats exhibited significant increases in both mEPSC amplitude (Fig. 4B; untrained, 13.9 ± 0.1 pA, 1-day trained, 15.9 ± 2.1 pA, 2-days trained, 17.5 ± 0.7 pA; $F_{(2,187)} = 7.21$; $P < 0.001$, one-way

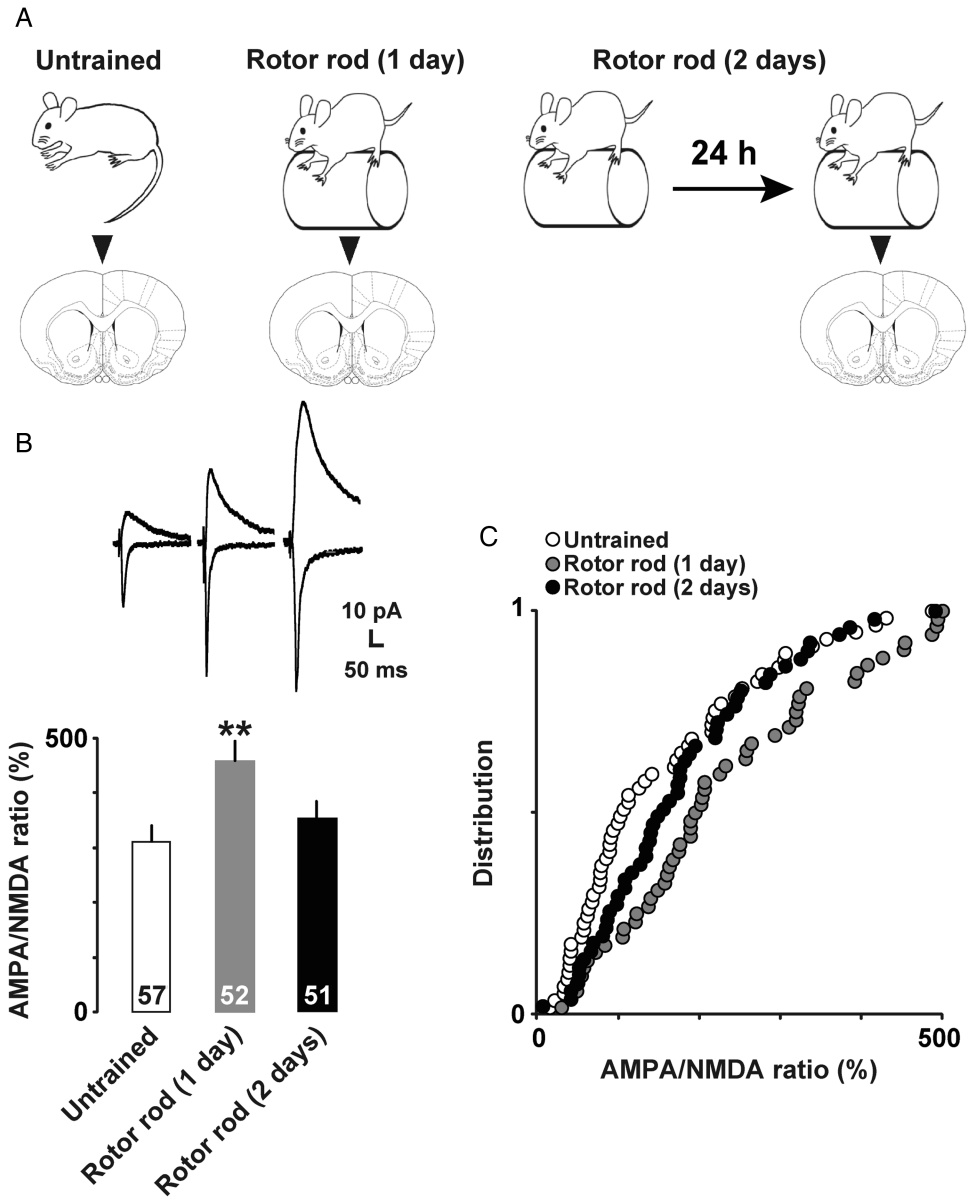


**Figure 2.** (*A*) Experimental design for patch clamp and Western blot. (*B*) Representative traces (upper) and mean AMPA/NMDA ratios (lower). $^{**}P < 0.01$ versus untrained. The number of neurons is shown at the bottom of each bar. Error bars indicate ± SEM. The number of neurons is shown at the bottom of each bar. (*C*) Cumulative distributions of AMPA/NMDA ratios of layer II/III neurons in untrained (open), 1-day trained (gray), and 2-days trained (filled) rats.

factorial ANOVA) and frequency (Fig. 4C; untrained, 49.3 ± 6.8 events/5 min, 1-day trained, 58.5 ± 13.7 events/5 min, 2-days trained, 84.8 ± 14.3 events/5 min; $F_{(2,187)} = 2.37$; $P = 0.042$, one-way factorial ANOVA). These results suggested that motor training increased the number of postsynaptic AMPA receptors. Within the same neuron, we sequentially measured mIPSCs at +15 mV. 1-day trained rats exhibited a significant decrease in mIPSC frequency (Fig. 4C; untrained, 292.1 ± 32.6 events/5 min, 1-day trained, 125.2 ± 12.3 events/5 min, 2-days trained, 276.9 ± 33.4 events/5 min; $F_{(2,\ 187)} = 9.24$; $P < 0.001$, one-way factorial ANOVA), while mIPSC amplitude did not significantly differ among groups (Fig. 4B; untrained, 30.5 ± 1.5 pA, 1-day trained, 30.1 ± 1.7 pA, 2-days trained, 30.3 ± 1.5; $F_{2,187} = 0.02$; $P = 0.98$, one-way factorial ANOVA). To analyze the similarities of amplitudes or frequencies between mEPSCs and mIPSCs, each mEPSC value was plotted against the mIPSC value (Fig. 4B and C). In both training groups, amplitudes were significantly correlated between mEPSCs and mIPSCs (Fig. 4B; untrained, $\rho = 0.20$, $P = 0.10$; 1-day trained, $\rho = 0.48$, $P < 0.001$; 2-days trained, $\rho = 0.28$, $P = 0.02$, Spearman's test), while frequencies were not correlated (Fig. 4C; untrained, $\rho = 0.18$, $P = 0.16$; 1-day trained, $\rho = 0.06$, $P = 0.63$; 2-days trained, $\rho = 0.15$, $P = 0.25$, Spearman's test). We recorded the data from a large number of cells to analyze a diversity of synaptic inputs and the correlation.

We further calculated the excitation and inhibition (E/I) balance for amplitude and frequency. The 2-days trained rats showed a significantly increased E/I balance for amplitude compared with that of the untrained rats (Fig. 4D; untrained, 0.54 ± 0.04, 1-day trained, 0.56 ± 0.03, 2-days trained, 0.66 ± 0.04; $H = 11.1$; $P = 0.002$, Kruskal–Wallis test). The E/I balance for frequency tended to increase in the 1-day trained rats, but decreased significantly in the 2-days trained rats (Fig. 4E; untrained, 0.72 ± 0.21, 1-day trained, 7.23 ± 5.11, 2-days trained, 0.50 ± 0.19; $H = 12.8$;

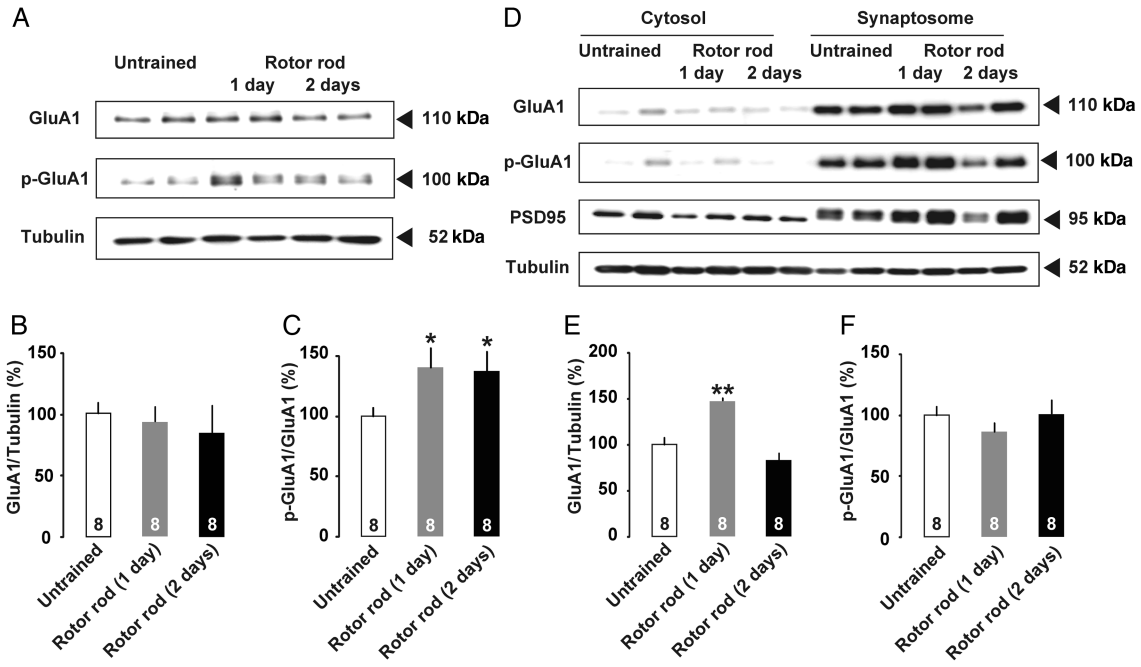


**Figure 3.** (*A*) Trimmed cortical tissues containing surface layers of M1 (layer I–III) were analyzed by Western blot. Molecular masses of standards are indicated on the right. (*B*) Total GluA1 was normalized to total β-Tubulin. (*C*) The phosphospecific signal of $Ser^{831}$ GluA1 was normalized to total GluA1. Motor training significantly increased $Ser^{831}$ phosphorylation in crude tissue extracts. (*D*) Western blot of cytosol and synaptosomal fraction. (*E*) Normalized GluA1 levels in the synaptosomal fraction were significantly increased in 1-day trained rats. (*F*) The phosphospecific signal of $Ser^{831}$ GluA1 normalized to total GluA1 did not change in the synaptosomal fraction. $^{*}P < 0.05$, $^{**}P < 0.01$ versus untrained. The number of rats in each group is shown at the bottom of each bar. Error bars indicate ± SEM.

$P = 0.017$, Kruskal–Wallis test). We further calculated the E/I balance deviation as the absolute value of the difference between the individual values and the mean value. The 1-day trained rats showed a significantly wider E/I deviation compared with the untrained or 2-days trained rats (Fig. 4F; untrained, 0.90 ± 0.18, 1-day trained, 12.55 ± 5.28, 2-days trained, 0.59 ± 0.16; $H = 126.4$; $P < 0.001$, Kruskal–Wallis test).

To examine presynaptic plasticity, we analyzed paired-pulse ratio after motor training. At the excitatory synapses, the paired-pulse ratio for evoked EPSCs was significantly decreased in 2-days trained rats, suggesting a long-term increase in presynaptic glutamate release probability (Fig. 5A; untrained, 0.70 ± 0.04, 1-day trained, 0.64 ± 0.03, 2-days trained, 0.57 ± 0.04; $F_{(2,85)} = 3.25$; $P = 0.044$, one-way factorial ANOVA; $P = 0.013$, Fisher's PLSD). Conversely, at the inhibitory synapses, the paired-pulse ratio for evoked IPSCs was significantly increased in 1-day trained rats, suggesting a transient decrease in the presynaptic GABA release probability (Fig. 5B; untrained, 0.67 ± 0.04, 1-day trained, 0.75 ± 0.05, 2-days trained, 0.66 ± 0.04; $F_{(2,118)} = 5.23$; $P = 0.007$, one-way factorial ANOVA; $P = 0.016$, Fisher's PLSD).

Finally, to investigate motor training-dependent intrinsic plasticity in M1 layer II/III neurons, we prepared acute brain slices for current clamp analyses. As shown in representative traces in Figure 6A, 1-day trained rats induced less spikes, but 2-days trained rats induced much more spikes than untrained rats. Figure 6B shows the relationship between current intensity and number of action potentials. Two-way repeated-measures ANOVA found the main effects of motor training ($F_{(2,2587)} = 29.82$; $P < 0.001$) and injected current ($F_{(13,2587)} = 483.63$; $P < 0.001$). Significant interaction was also observed between training and current ($F_{(26,2587)} = 24.01$; $P < 0.001$). Compared with untrained control, post hoc ANOVA showed less number of spikes in 1-day trained rats ($F_{(1,1664)} = 9.78$; $P = 0.002$), while more spikes were observed in 2-days trained rats ($F_{(1,1755)} = 18.68$; $P < 0.001$).

The 2-days trained rats also showed a significant increase in resting membrane potential compared with other groups (Fig. 6C; untrained, −71.0 ± 0.6 mV, 1-day trained, −72.7 ± 0.5 mV, 2-days trained, −68.7 ± 0.7 mV; $F_{(2,199)} = 11.5$; $P < 0.001$, one-way factorial ANOVA; $P = 0.007$, Fisher's PLSD). The threshold was also significantly increased in the 1-day trained rats compared with untrained rats (Fig. 6C; untrained, −34.8 ± 1.0 mV, 1-day trained, −30.4 ± 1.0 mV, 2-days trained, −36.5 ± 1.1 mV; $F_{(2,199)} = 9.51$; $P < 0.001$, one-way factorial ANOVA; $P = 0.003$, Fisher's PLSD). Moreover, the 1-day trained rats exhibited the largest AHP amplitude (Fig. 6C; untrained, −5.2 ± 0.5 mV, 1-day trained, −9.4 ± 0.5 mV, 2-days trained, −5.3 ± 0.3 mV; $F_{(2,199)} = 30.9$; $P < 0.001$, one-way factorial ANOVA; $P < 0.001$, Fisher's PLSD). Membrane resistance was significantly increased in the 2-days trained rats (Fig. 6D; untrained, 69.6 ± 4.5 MΩ, 1-day trained, 76.2 ± 3.7 MΩ, 2-days trained, 86.8 ± 5.9 MΩ; $F_{(2,199)} = 3.26$; $P = 0.040$, one-way factorial ANOVA; $P = 0.013$, Fisher's PLSD), while the groups did not significantly differ with regard to series resistance (Fig. 6D; $F_{(2,199)} = 0.66$; $P = 0.51$, one-way factorial ANOVA) and membrane capacitance (data not shown; $F_{(2,199)} = 1.63$; $P = 0.16$, one-way factorial ANOVA).

To investigate whether AMPA and/or NMDA receptor mediate the intrinsic plasticity, we microinjected vehicle, CNQX, or APV before the motor training in 1-day trained rats. As shown in representative traces in Figure 7A, pretreatment of CNQX or APV induced more spikes than vehicle-injected 1-day trained rats, suggesting AMPA and/or NMDA receptor-mediated the intrinsic plasticity. Figure 7B shows the relationship between current intensity and number of action potentials. Two-way repeated-measures ANOVA found the main effects of drug ($F_{(2,1053)} = 7.74$; $P < 0.001$) and injected current ($F_{(13,1053)} = 161.02$; $P < 0.001$). Significant interaction was also observed between drug and current ($F_{(26,1053)} = 5.99$; $P < 0.001$). Compared with vehicle injected rats, post hoc ANOVA showed significant increase in the number

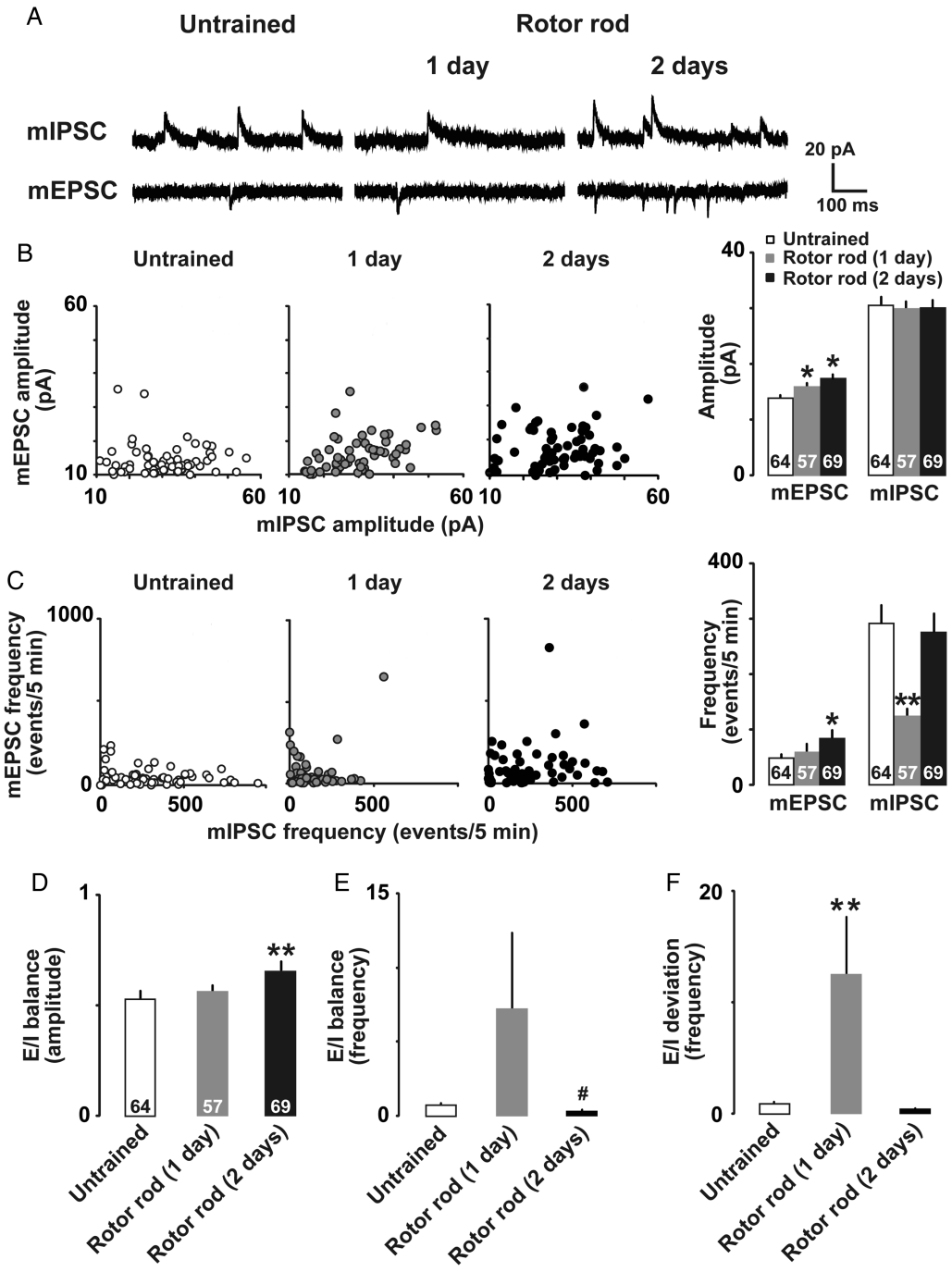


**Figure 4.** (*A*) Representative traces of mEPSCs and mIPSCs in M1 layer II/III neurons. (*B*) Plots of mEPSC and mIPSC amplitudes in untrained (open), 1-day trained (gray), and 2-days trained (filled) rats. (*C*) Plots of mEPSC and mIPSC frequencies. (*D*) E/I balance for the amplitude, (*E*) frequency, and (*F*) deviation of E/I balance for frequency. $^{*}P < 0.05$, $^{**}P < 0.01$ versus untrained. $^{\#}P < 0.05$ versus 1-day trained. The number of neurons is shown at the bottom of each bar. Error bars indicate ± SEM.

of spikes in CNQX ($F_{(1,\ 702)} = 9.86$; $P = 0.003$) or APV injected rats ($F_{(1,\ 702)} = 14.44$; $P < 0.001$).

Although neither drug affects the resting membrane potential (Fig. 7*C*; vehicle, −71.4 ± 0.6 mV, CNQX, −69.4 ± 1.2 mV, APV, −68.6 ± 1.7 mV; $F_{(2,\ 81)} = 1.40$; $P = 0.25$, one-way factorial ANOVA), CNQX injected rats showed significantly lower threshold (Fig. 7*C*; vehicle, −21.0 ± 1.7 mV, CNQX, −28.0 ± 1.2 mV, APV, −24.8 ± 2.6 mV; $F_{(2,81)} = 3.13$; $P = 0.048$, one-way factorial ANOVA; $P = 0.014$, Fisher's PLSD) and higher AHP amplitude (Fig. 7*C*; vehicle, −10.5 ± 0.9 mV, CNQX, −7.6 ± 1.2 mV, APV, −7.3 ± 0.8 mV; $F_{(2,81)} = 3.29$; $P = 0.04$, one-way factorial ANOVA; $P = 0.039$ for CNQX, $P = 0.023$ for APV, Fisher's PLSD) than vehicle injected rats. Both CNQX and APV injected rats showed significantly higher membrane resistance than vehicle injected rats (Fig. 7*D*; vehicle, 50.5 ± 3.8 MΩ, CNQX, 77.2 ± 7.8 MΩ, APV, 83.3 ± 8.3 MΩ; $F_{(2,199)} = 6.49$; $P = 0.0024$, one-way factorial ANOVA; $P = 0.007$ for CNQX, $P = 0.001$ for APV, Fisher's PLSD), while neither drug affected the series resistance (Fig. 7*D*; $F_{(2,83)} = 0.93$; $P = 0.40$, one-way factorial

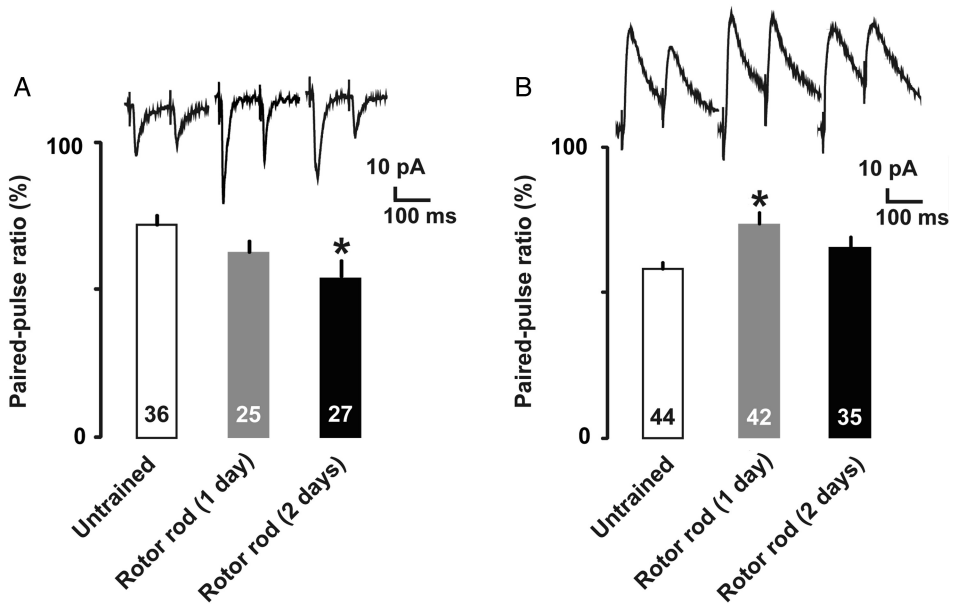


**Figure 5.** (*A*) Representative traces of paired-pulse responses with a 100-ms inter-stimulus interval. AMPA receptor-mediated paired-pulse ratio in untrained (open), 1-day trained (gray), and 2-days trained (filled) rats. (*B*) Representative traces and $GABA_A$ receptor-mediated paired-pulse response. *$P < 0.05$ versus untrained. The number of neurons is shown at the bottom of each bar. Error bars indicate ± SEM.

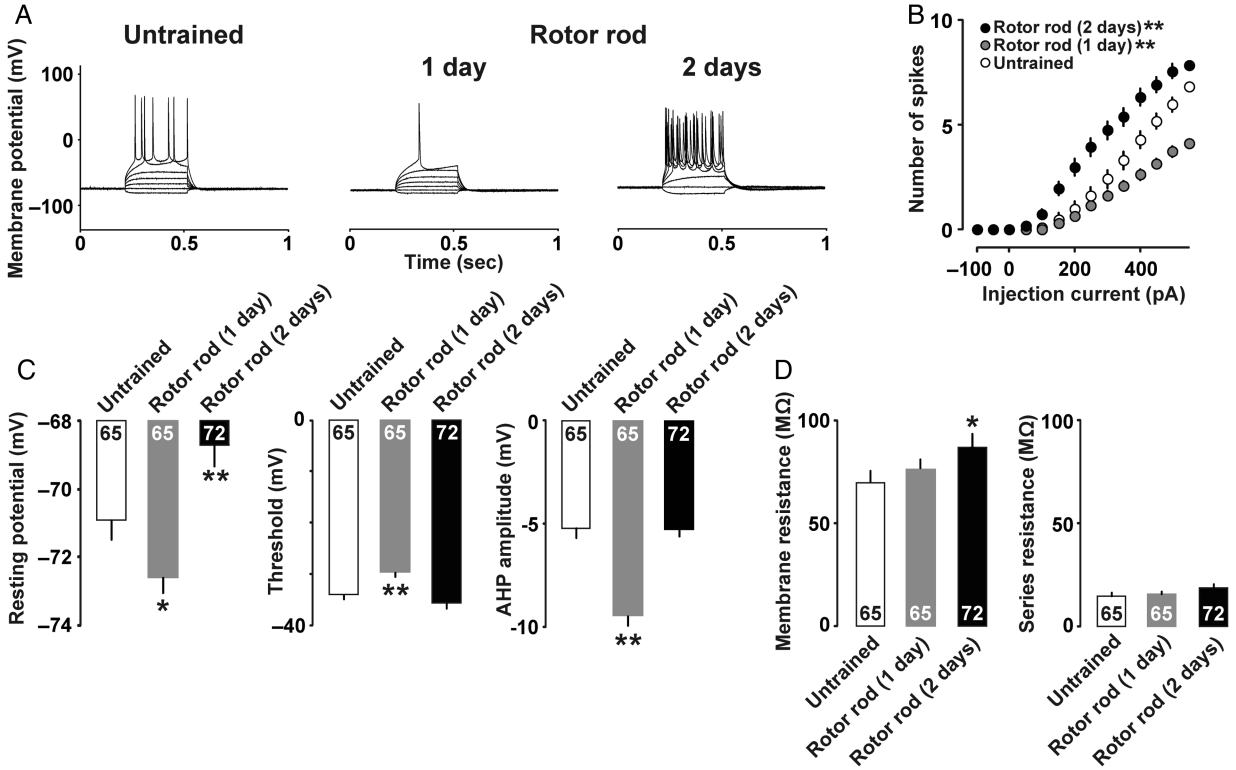


**Figure 6.** (*A*) Example traces of action potentials induced by current injections. (*B*) Mean input/output relationship in untrained (open), 1-day trained (gray), and 2-days trained (filled) rats. (*C*) Mean resting membrane potentials, threshold, and amplitude of the AHP. (*D*) Mean membrane resistance and series resistance. *$P < 0.05$, **$P < 0.01$ versus untrained. The number of neurons is shown at the bottom of each bar. Error bars indicate ± SEM.

ANOVA). Both CNQX and APV injected rats showed significantly lower membrane capacitance than vehicle injected rats (data not shown; $F_{(2,83)} = 5.04$; $P = 0.009$, one-way factorial ANOVA).

Compared with the uninjected group (1-day trained in Fig. 6*D*), vehicle injection seems to increase the threshold of action potential and decrease the membrane resistance (Fig. 7*D*), which is

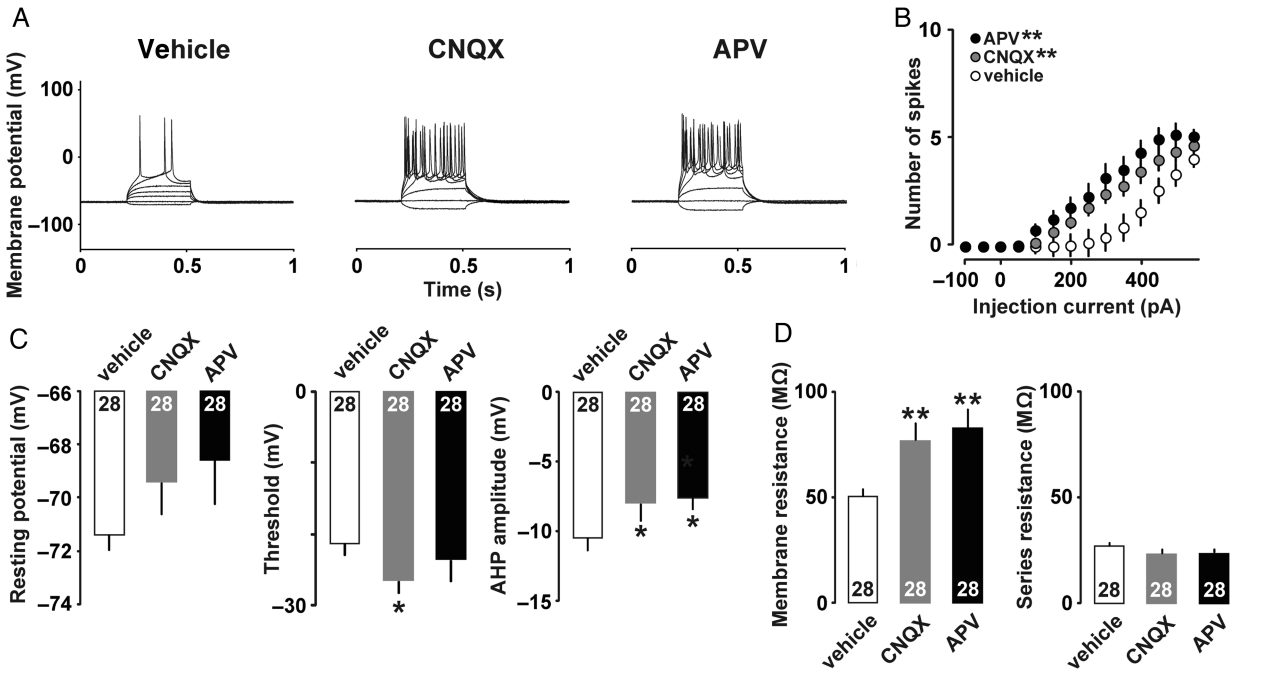


**Figure 7.** (*A*) Example traces of action potentials in 1-day trained rats. Either vehicle, CNQX, or APV was microinjected into the M1 before the first trial. (*B*) Mean input/output relationship in vehicle (open), CNQX (gray), and APV (filled). (*C*) Mean resting membrane potentials, threshold, and amplitude of the AHP. (*D*) Mean membrane resistance and series resistance. $^{*}P < 0.05$, $^{**}P < 0.01$ versus vehicle. The number of neurons is shown at the bottom of each bar. Error bars indicate ± SEM.

known to affect the membrane excitability (Perkins 2006; Kandel et al. 2012).

## Discussion

### Role of Glutamatergic Transmission in the M1

We confirmed the role of glutamatergic transmission of the M1 in motor skill performance in Figure 1. Bilateral microinjection of CNQX immediately after motor skill acquisition impaired the motor performance, suggesting that AMPA receptor activation is necessary to maintain acquired motor skills (Fig. 1*D*). Since the transient effect of CNQX did not affect open field performance (Fig. 1*G*), it is possible that AMPA receptor-mediated glutamatergic transmission in the M1 is closely associated with the acquired motor skill rather than the basic motor activity.

Conversely, bilateral microinjection of either APV or CNQX prior to motor skill acquisition successfully impaired motor performance, suggesting that motor skill acquisition requires both NMDA and AMPA receptors. In support of this, mice lacking NMDA receptor specifically in the M1 (*Grin1*-v$\Delta^{MCx}$) showed clear impairment of conditioned eye-blink responses (Hasan et al. 2013).

CNQX microinjections prior to the motor training exhibited longer effect for motor learning (Fig. 1*H*). In contrast, the microinjections after the training attenuated the performance transiently (Fig. 1*D*). These findings led us the hypothesis that microinjections of CNQX or APV before the training may block the calcium triggered plasticity and learning, while activated postsynaptic AMPA receptor turnover after training may shorten the effect of CNQX. To prove the hypothesis, further study is necessary to compare the AMPA receptor recycling and insertion of AMPA receptors (Park et al. 2004; Petrini et al. 2009) before and after the motor training.

### Glutamatergic Plasticity

Motor training induces LTP in M1 layer II/III neurons (Rioult-Pedotti et al. 2000; Harms et al. 2008), but little is known regarding the detailed mechanisms of plasticity at the synapse level. To investigate this subject, we analyzed synaptic plasticity in layer II/III neurons using a voltage clamp technique. The 1-day trained rats showed an increased amplitude but not frequency of mEPSCs, suggesting increased postsynaptic AMPA receptors in the early phase of motor learning. On the other hand, the 2-days trained rats showed an increase in mEPSC frequency and a decrease in paired-pulse ratio, suggesting increased presynaptic glutamate release during the late phase of learning.

Previous studies reveal that AMPA receptor phosphorylation is induced by calcium/calmodulin-dependent protein kinase II for AMPA receptor delivery (Fukunaga et al. 1996; Shi et al. 2001; Malinow and Malenka 2002). Our Western blot results showed increased $Ser^{831}$ phosphorylation of the AMPA receptor GluA1 subunit at 30 min, and synaptosomal GluA1 subunit in 1-day trained rats, suggesting that acute motor training induced AMPA receptor delivery into the excitatory synapses. Consistently, mice trained forelimb reaching task increased synaptosomal GluA1 in the forelimb region of the motor cortex (Padmashri et al. 2013).

Morphologically, quantitative electron microscopy indicated an increased number of synapses per neuron after motor training (Kleim et al. 2004). Moreover, previous in vivo imaging studies clearly show rapid synapse formation and stabilization after motor training in mice expressing YFP neurons (Xu et al. 2009; Yang et al. 2009). Using GluA1 subunit tagged with a pH-sensitive form of GFP (SEP-GluA1), Zhang et al. (2015) further demonstrated dynamic insertion of the subunit at dendritic spines in the barrel cortex after the somatosensory experiences. Although the morphological dynamics is still unknown in the motor cortex, present data provide a functional evidence of plasticity at excitatory synapses after motor training. In addition to motor training

induced increases in AMPA receptor response (Fig. 4B), we found long-term increase in presynaptic glutamate release probability in 2-days trained rats (Fig. 5A).

### GABAergic Plasticity

After motor training, we observed $GABA_A$ receptor-mediated inhibitory plasticity at the synapses of M1 layer II/III. The decreased mIPSC frequency and increased paired-pulse ratio in the 1-day trained rats suggest a decreased presynaptic GABA release probability during the early stage of training. While a drastic increase in E/I balance may cause seizures, a transient decrease in resting membrane potential seems to prevent increased neural activity in 1-day trained rats. Interestingly, the transient reduction of GABAergic inhibition appears consistent with human studies in which magnetic resonance spectroscopy shows a reduced GABA concentration in the M1 during the acute learning stage (Floyer-Lea et al. 2006; Stagg et al. 2011). Moreover, in vivo 2-photon imaging study further demonstrated subtype-specific rapid elimination of inhibitory boutons on distal dendrites of layer II/III neurons after motor training: somatostatin- but not parvalbumin-expressing GABAergic neurons decrease the axonal boutons immediately after the motor training began (Chen et al. 2015).

Since transient suppression of local $GABA_A$ inhibition is necessary for long-term potentiation (LTP) in the motor cortex (Hess and Donoghue 1994; Castro-Alamancos et al. 1995), the decrease in GABA release probability may promote AMPA receptor-mediated plasticity for motor skill learning in 1-day trained rats. Then, 2-days trained rats restored the GABA release probability and balanced E/I ratio. Although the role of the long-term plasticity of both inhibitory and excitatory synapses is still unknown, it may contribute to the reorganization of central motor representation of M1 after skill training (Karni et al. 1995; Classen et al. 1998; Kleim et al. 1998).

We also identified a significant relationship between mEPSC and mIPSC amplitude after motor learning. This observation seems consistent with previous findings in the prefrontal cortex (Haider et al. 2006) and the hippocampus (Mitsushima et al. 2013). Since contextual training slightly decreased presynaptic glutamate release probability at hippocampal CA1 synapses (Mitsushima et al. 2013), the styles of learning-induced plasticity seems to vary among different brain areas and different types of learning.

The transient decrease in GABAergic inhibition after 1 day of training may increase seizure risk. Exercise acutely increases neural activity in the cortex and, thus, physical exercise has been discouraged for patients with epilepsy (Ogunyemi et al. 1988; Simpson and Grossman 1989). However, considerable evidence also suggests that exercise does not always trigger epileptic seizure (Roth et al. 1994; Nakken 1999), since long-term exercise instead helps to prevent such seizures (Peixinho-Pena et al. 2012; Pimentel et al. 2015). Although many papers focused on the exercise-induced seizures, it is possible that the first step of plasticity (disinhibition from GABA) acutely increases a risk of seizure. Considering the importance of GABA/glutamate balance as a cause of seizure (Bradford 1995; Rassner et al. 2016), large clinical study about the skill training and seizure may help us to understand the disease mechanism.

### Changes in Intrinsic Properties

Using current clamp technique, we examined changes in the intrinsic properties of M1 layer II/III neurons after motor training. The 1-day trained rats showed significantly decreased resting membrane potential, and increases of both spike threshold and amplitude of AHP. The 2-days trained rats exhibited significantly increased resting membrane potential, leading to increased excitability. Repeated evoked firing of M1 neurons induces a long-term increase in membrane excitability in approximately 70% of neurons (Debanne 2009; Paz et al. 2009), and here we revealed detailed changes in membrane properties after motor training. Moreover, the high membrane excitability in the 2-days trained rats seems consistent with human studies showing that a decreased motor threshold increases neural activity in the late phase of motor learning (Muellbacher et al. 2001; Delvendahl et al. 2012). The training-dependent changes in both membrane potential and resistance may be specific to the M1 area, since operant conditioning tasks do not affect resting membrane potential or resistance in the piriform cortex (Saar et al. 1998).

It remains unknown what controls the membrane potential and membrane resistance. One candidate is TREK-1, a 2-pore-domain potassium channel that controls the resting membrane potential in the brain (Thomas and Goldstein 2009; Ji et al. 2011). Since TREK-1 channel expression results in lower resting membrane potential (Honoré 2007), the drastic changes in intrinsic neuronal properties during the early phase of motor learning may depend on potassium currents. Additionally, increased intracellular calcium opens calcium-dependent potassium (KCa) channels, inducing membrane hyperpolarization (Kaczorowski and Garcia 1999; Stackman et al. 2002; Bond et al. 2004). Moreover, a recent study demonstrated that KCa channel overexpression reduces input resistance (Garcia-Junco-Clemente et al. 2013). Thus, the activation of TREK1 and/or KCa channels may be responsible for changing the resting membrane potential immediately after motor training.

We also found that the spike threshold was transiently increased in the 1-day trained rats, although the mechanism remains unclear. Potassium current mediated by low-threshold voltage-gated potassium channels ($K_v1$, $K_v4$, and $K_v7$) reportedly increases the spike threshold (Yuan et al. 2005; Guan et al. 2007; Shah et al. 2008), while sodium channel subunit $Na_v1.6$ may play a role in lowering the action potential threshold (Royeck et al. 2008). Motor training could acutely increase the potassium channel expression, or decrease the sodium channel expression in layer II/III neurons.

To test whether AMPA or NMDA receptors mediates the changes in the intrinsic excitability, we performed current clamp studies in Figure 7. The pretreatment of CNQX or APV successfully blocked the transient decrease in intrinsic excitability in 1-day trained rats, suggesting that the changes of intrinsic excitability in M1 layer II/III neurons requires activation of both AMPA and NMDA receptors. Blockade of learning-induced transmission by CNQX or APV may increase the excitability in M1 pyramidal neurons in 1-day trained rats, since long-term activity blockade increases the firing rate and spike threshold in cortical pyramidal neurons (Desai et al. 1999). Moreover, NMDA- or non-NMDA receptor-mediated frequent EPSCs (50 Hz) is known to evoke slow $Ca^{2+}$-dependent $K^+$ current AHP in pyramidal neurons (Lancaster et al. 2001). Although it has been unknown whether the training-dependent glutamatergic stimulation induces the AHP, the decrease in the AHP in 1-day trained rats seems to require the activation of both AMPA and NMDA receptors in M1 layer II/III neurons.

## Conclusion

Our present results revealed dynamic changes in synaptic plasticity and neural properties after motor training within M1, which is traditionally considered an output area for voluntary movements. In the 1-day trained rats, motor training strengthened

AMPA receptor-mediated excitatory synapses and drastically reduced presynaptic GABA release probability. Moreover, these animals showed a higher threshold and lower resting membrane potential compared with untrained controls, which may contribute to the homeostatic regulation of firing rates in 1-day trained rats. In the 2-days trained rats, motor training further strengthened AMPA receptor-mediated excitatory synapses together with NMDA receptors and increased presynaptic glutamate release, while increasing the presynaptic GABA release probability. Additionally, E/I balance, threshold, and resting membrane potential decreased to the levels in untrained controls. Based on our findings, we conclude that motor training promotes synaptic plasticity at both excitatory and inhibitory synapses, as well as changes neural properties, such as resting membrane potential and threshold of M1 layer II/III neurons.

## Funding

This project was supported by Grants-in-Aid for Young Scientists (H.K.), Scientific Research B (D.M.), Scientific Research C (D.M.), and Scientific Research on Innovative Areas (D.M.) from the Ministry of Education, Culture, Sports, Science and Technology of Japan. Grants-in-Aid from the Nakatomi Foundation (H.K.), Meiji Yasuda Life Foundation of Health and Welfare (H.K.), Yokohama Foundation of Advancement of Medical Science (D.M.), and Yokohama Academic Foundation (D.M.) also support the project. Funding to pay the Open Access publication charges for this article was provided by the grant-in-aid for scientific research.

## Notes

We would like to thank Dr Y. Sakimoto and Dr T. Inoue for helpful comments and suggestions. *Conflict of Interest*: None of the authors has any conflict of interest to disclose. We confirm that we have read the Journal's position on issues involved in ethical publication, and we affirm that this report is consistent with those guidelines. The funders had no role in study design, data collection and analysis, decision to publish, or preparation of the manuscript.

## References

Baidan LV, Zholos AV, Wood JD. 1995. Modulation of calcium currents by G-proteins and adenosine receptors in myenteric neurones cultured from adult guinea-pig small intestine. Br J Pharmacol. 116:1882–1886.

Bond CT, Herson PS, Strassmaier T, Hammond R, Stackman R, Maylie J, Adelman JP. 2004. Small conductance $Ca^{2+}$-activated $K^{+}$ channel knock-out mice reveal the identity of calcium-dependent afterhyperpolarization currents. J Neurosci. 24: 5301–5306.

Bradford HF. 1995. Glutamate, GABA and epilepsy. Prog Neurobiol. 47:477–511.

Caillard O, Ben-Ari Y, Gaiarsa JL. 1999. Long-term potentiation of GABAergic synaptic transmission in neonatal rat hippocampus. J Physiol. 518(Pt 1):109–119.

Cantarero G, Lloyd A, Celnik P. 2013. Reversal of long-term potentiation-like plasticity processes after motor learning disrupts skill retention. J Neurosci. 33:12862–12869.

Castro-Alamancos MA, Donoghue JP, Connors BW. 1995. Different forms of synaptic plasticity in somatosensory and motor areas of the neocortex. J Neurosci. 15:5324–5333.

Chen SX, Kim AN, Peters AJ, Komiyama T. 2015. Subtype-specific plasticity of inhibitory circuits in motor cortex during motor learning. Nat Neurosci. 18:1109–1115.

Classen J, Liepert J, Wise SP, Hallett M, Cohen LG. 1998. Rapid plasticity of human cortical movement representation induced by practice. J Neurophysiol 79:1117–1123.

Cui Y, Costa RM, Murphy GG, Elgersma Y, Zhu Y, Gutmann DH, Parada LF, Mody I, Silva AJ. 2008. Neurofibromin regulation of ERK signaling modulates GABA release and learning. Cell 135:549–560.

Daoudal G, Debanne D. 2003. Long-term plasticity of intrinsic excitability: learning rules and mechanisms. Learn Mem. 10:456–465.

Debanne D. 2009. Plasticity of neuronal excitability in vivo. J Physiol. 587:3057–3058.

Delvendahl I, Jung NH, Kuhnke NG, Ziemann U, Mall V. 2012. Plasticity of motor threshold and motor-evoked potential amplitude–a model of intrinsic and synaptic plasticity in human motor cortex? Brain Stimul. 5:586–593.

Desai NS, Rutherford LC, Turrigiano GG. 1999. Plasticity in the intrinsic excitability of cortical pyramidal neurons. Nat Neurosci. 2:515–520.

Evarts EV. 1968. Relation of pyramidal tract activity to force exerted during voluntary movement. J Neurophysiol. 31:14–27.

Floyer-Lea A, Wylezinska M, Kincses T, Matthews PM. 2006. Rapid modulation of GABA concentration in human sensorimotor cortex during motor learning. J Neurophysiol. 95:1639–1644.

Fukunaga K, Muller D, Miyamoto E. 1996. CaM kinase II in long-term potentiation. Neurochem Int. 28:343–358.

Garcia-Junco-Clemente P, Chow DK, Tring E, Lazaro MT, Trachtenberg JT, Golshani P. 2013. Overexpression of calcium-activated potassium channels underlies cortical dysfunction in a model of PTEN-associated autism. Proc Natl Acad Sci U S A. 110:18297–18302.

Georgopoulos AP, Kalaska JF, Caminiti R, Massey JT. 1982. On the relations between the direction of two-dimensional arm movements and cell discharge in primate motor cortex. J Neurosci. 2:1527–1537.

Guan D, Lee JC, Higgs MH, Spain WJ, Foehring RC. 2007. Functional roles of Kv1 channels in neocortical pyramidal neurons. J Neurophysiol. 97:1931–1940.

Haider B, Duque A, Hasenstaub AR, McCormick DA. 2006. Neocortical network activity in vivo is generated through a dynamic balance of excitation and inhibition. J Neurosci. 26:4535–4545.

Harms KJ, Rioult-Pedotti MS, Carter DR, Dunaevsky A. 2008. Transient spine expansion and learning-induced plasticity in layer 1 primary motor cortex. J Neurosci. 28:5686–5690.

Hasan MT, Hernández-Gonzalez S, Dogbevia G, Treviño M, Bertocchi I, Gruart A, Delgado-García JM. 2013. Role of motor cortex NMDA receptors in learning-dependent synaptic plasticity of behaving mice. Nat Commun. doi: 10.1038/ncomms3258.

Hess G, Donoghue JP. 1994. Long-term potentiation of horizontal connections provides a mechanism to reorganize cortical motor maps. J Neurophysiol. 71:2543–2547.

Honoré E. 2007. The neuronal background $K_{2P}$ channels: focus on TREK1. Nat Rev Neurosci. 8:251–261.

Ji XC, Zhao WH, Cao DX, Shi QQ, Wang XL. 2011. Novel neuroprotectant chiral 3-n-butylphthalide inhibits tandem-pore-domain potassium channel TREK-1. Acta Pharmacol Sin. 32:182–187.

Kaczorowski GJ, Garcia ML. 1999. Pharmacology of voltage-gated and calcium-activated potassium channels. Curr Opin Chem Biol. 3:448–458.

Kandel E, Schwartz J, Jessell T, Siegelbaum S, Hudspeth AJ. 2012. Principles of Neural Science. 5th ed. Chapter 6, McGraw-Hill Education.

Kaneko T. 2013. Local connections of excitatory neurons in motor-associated cortical areas of the rat. Front Neural Circuits. 7:75.

Karni A, Meyer G, Jezzard P, Adams MM, Turner R, Ungerleider LG. 1995. Functional MRI evidence for adult motor cortex plasticity during motor skill learning. Nature. 377:155–158.

Kleim JA, Barbay S, Cooper NR, Hogg TM, Reidel CN, Remple MS, Nudo RJ. 2002. Motor learning-dependent synaptogenesis is localized to functionally reorganized motor cortex. Neurobiol Learn Mem. 77:63–77.

Kleim JA, Barbay S, Nudo RJ. 1998. Functional reorganization of the rat motor cortex following motor skill learning. J Neurophysiol. 80:3321–3325.

Kleim JA, Hogg TM, VandenBerg PM, Cooper NR, Bruneau R, Remple M. 2004. Cortical synaptogenesis and motor map reorganization occur during late, but not early, phase of motor skill learning. J Neurosci. 24:628–633.

Kurotani T, Yamada K, Yoshimura Y, Crair MC, Komatsu Y. 2008. State-dependent bidirectional modification of somatic inhibition in neocortical pyramidal cells. Neuron 57:905–916.

Lancaster B, Hu H, Ramakers GM, Storm JF. 2001. Interaction between synaptic excitation and slow afterhyperpolarization current in rat hippocampal pyramidal cells. J Physiol. 536:809–823.

Lee HK, Takamiya K, Han JS, Man H, Kim CH, Rumbaugh G, Yu S, Ding L, He C, Petralia RS, et al. 2003. Phosphorylation of the AMPA receptor GluR1 subunit is required for synaptic plasticity and retention of spatial memory. Cell 112:631–643.

Liu G. 2004. Local structural balance and functional interaction of excitatory and inhibitory synapses in hippocampal dendrites. Nat Neurosci. 7:373–379.

Ma L, Qiao Q, Tsai JW, Yang G, Li W, Gan WB. 2016. Experience-dependent plasticity of dendritic spines of layer 2/3 pyramidal neurons in the mouse cortex. Dev Neurobiol. 76:277–286.

Malinow R, Malenka RC. 2002. AMPA receptor trafficking and synaptic plasticity. Annu Rev Neurosci. 25:103–126.

Mitsushima D, Ishihara K, Sano A, Kessels HW, Takahashi T. 2011. Contextual learning requires synaptic AMPA receptor delivery in the hippocampus. Proc Natl Acad Sci U S A. 108:12503–12508.

Mitsushima D, Sano A, Takahashi T. 2013. A cholinergic trigger drives learning-induced plasticity at hippocampal synapses. Nat Commun. doi: 10.1038/ncomms3760.

Mitsushima D, Takase K, Funabashi T, Kimura F. 2009. Gonadal steroids maintain 24 h acetylcholine release in the hippocampus: organizational and activational effects in behaving rats. J Neurosci. 29:3808–3815.

Moran DW, Schwartz AB. 1999. Motor cortical representation of speed and direction during reaching. J Neurophysiol. 82:2676–2692.

Moyer JR Jr., Thompson LT, Disterhoft JF. 1996. Trace eyeblink conditioning increases CA1 excitability in a transient and learning-specific manner. J Neurosci. 16:5536–5546.

Muellbacher W, Ziemann U, Boroojerdi B, Cohen L, Hallett M. 2001. Role of the human motor cortex in rapid motor learning. Exp Brain Res. 136:431–438.

Nakken KO. 1999. Physical exercise in outpatients with epilepsy. Epilepsia 40:643–651.

Neafsey EJ, Bold EL, Haas G, Hurley-Gius KM, Quirk G, Sievert CF, Terreberry RR. 1986. The organization of the rat motor cortex: a microstimulation mapping study. Brain Res. 396:77–96.

Ogunyemi AO, Gomez MR, Klass DW. 1988. Seizures induced by exercise. Neurology 38:633–634.

Padmashri R, Reiner BC, Suresh A, Spartz E, Dunaevsky A. 2013. Altered structural and functional synaptic plasticity with motor skill learning in a mouse model of fragile X syndrome. J Neurosci. 33:19715–19723.

Park M, Penick EC, Edwards JG, Kauer JA, Ehlers MD. 2004. Recycling endosomes supply AMPA receptors for LTP. Science 305:1972–1975.

Paxinos G, Watson C. 1998. The Rat Brain in Stereotaxic Coordinates. 4th ed. San Diego: Academic Press.

Paz JT, Mahon S, Tiret P, Genet S, Delord B, Charpier S. 2009. Multiple forms of activity-dependent intrinsic plasticity in layer V cortical neurones in vivo. J Physiol. 587:3189–3205.

Peixinho-Pena LF, Fernandes J, de Almeida AA, Novaes Gomes FG, Cassilhas R, Venancio DP, de Mello MT, Scorza FA, Cavalheiro EA, Arida RM. 2012. A strength exercise program in rats with epilepsy is protective against seizures. Epilepsy Behav. 25:323–328.

Perkins KL. 2006. Cell-attached voltage-clamp and current-clamp recording and stimulation techniques in brain slices. J Neurosci Methods. 154:1–18.

Petrini EM, Lu J, Cognet L, Lounis B, Ehlers MD, Choquet D. 2009. Endocytic trafficking and recycling maintain a pool of mobile surface AMPA receptors required for synaptic potentiation. Neuron 63:92–105.

Pimentel J, Tojal R, Morgado J. 2015. Epilepsy and physical exercise. Seizure 25:87–94.

Rassner MP, Moser A, Follo M, Joseph K, van Velthoven-Wurster V, Feuerstein TJ. 2016. Neocortical GABA release at high intracellular sodium and low extracellular calcium: an anti-seizure mechanism? J Neurochem. doi: 10.1111/jnc.13555.

Riedel G, Platt B, Micheau J. 2003. Glutamate receptor function in learning and memory. Behav Brain Res. 140:1–47.

Rioult-Pedotti MS, Friedman D, Donoghue JP. 2000. Learning-induced LTP in neocortex. Science 290:533–536.

Rioult-Pedotti MS, Friedman D, Hess G, Donoghue JP. 1998. Strengthening of horizontal cortical connections following skill learning. Nat Neurosci. 1:230–234.

Roth DL, Goode KT, Williams VL, Faught E. 1994. Physical exercise, stressful life experience, and depression in adults with epilepsy. Epilepsia 35:1248–1255.

Royeck M, Horstmann MT, Remy S, Reitze M, Yaari Y, Beck H. 2008. Role of axonal NaV1.6 sodium channels in action potential initiation of CA1 pyramidal neurons. J Neurophysiol. 100: 2361–2380.

Saar D, Barkai E. 2003. Long-term modifications in intrinsic neuronal properties and rule learning in rats. Eur J Neurosci. 17:2727–2734.

Saar D, Grossman Y, Barkai E. 1998. Reduced after-hyperpolarization in rat piriform cortex pyramidal neurons is associated with increased learning capability during operant conditioning. Eur J Neurosci. 10:1518–1523.

Shah MM, Migliore M, Valencia I, Cooper EC, Brown DA. 2008. Functional significance of axonal Kv7 channels in hippocampal pyramidal neurons. Proc Natl Acad Sci U S A. 105: 7869–7874.

Shi S, Hayashi Y, Esteban JA, Malinow R. 2001. Subunit-specific rules governing AMPA receptor trafficking to synapses in hippocampal pyramidal neurons. Cell 105:331–343.

Shi SH, Hayashi Y, Petralia RS, Zaman SH, Wenthold RJ, Svoboda K, Malinow R. 1999. Rapid spine delivery and redistribution of AMPA receptors after synaptic NMDA receptor activation. Science 284:1811–1816.

Simpson RK Jr., Grossman RG. 1989. Seizures after jogging. N Engl J Med. 321:835.

Stackman RW, Hammond RS, Linardatos E, Gerlach A, Maylie J, Adelman JP, Tzounopoulos T. 2002. Small conductance $Ca^2$

$^{+}$-activated $K^{+}$ channels modulate synaptic plasticity and memory encoding. J Neurosci. 22:10163–10171.

Stagg CJ, Bachtiar V, Johansen-Berg H. 2011. The role of GABA in human motor learning. Curr Biol. 21:480–484.

Takahashi T, Svoboda K, Malinow R. 2003. Experience strengthening transmission by driving AMPA receptors into synapses. Science 299:1585–1588.

Takumi Y, Ramirez-Leon V, Laake P, Rinvik E, Ottersen OP. 1999. Different modes of expression of AMPA and NMDA receptors in hippocampal synapses. Nat Neurosci. 2:618–624.

Thomas D, Goldstein S. 2009. Two-P-domain ($K_{2P}$) potassium channels: leak conductance regulators of excitability. Encyclopedia of Neuroscience. Oxford: Academic Press. p. 1207–1220.

van der Velden L, van Hooft JA, Chameau P. 2012. Altered dendritic complexity affects firing properties of cortical layer 2/3 pyramidal neurons in mice lacking the 5-HT3A receptor. J Neurophysiol. 108:1521–1528.

Watt AJ, Sjostrom PJ, Hausser M, Nelson SB, Turrigiano GG. 2004. A proportional but slower NMDA potentiation follows AMPA potentiation in LTP. Nat Neurosci. 7:518–524.

Whitlock JR, Heynen AJ, Shuler MG, Bear MF. 2006. Learning induces long-term potentiation in the hippocampus. Science 313:1093–1097.

Xu T, Yu X, Perlik AJ, Tobin WF, Zweig JA, Tennant K, Jones T, Zuo Y. 2009. Rapid formation and selective stabilization of synapses for enduring motor memories. Nature 462:915–919.

Yamamoto Y, Shioda N, Han F, Moriguchi S, Fukunaga K. 2013. Novel cognitive enhancer ST101 enhances acetylcholine release in mouse dorsal hippocampus through T-type voltage-gated calcium channel stimulation. J Pharmacol Sci. 121: 212–226.

Yang G, Pan F, Gan WB. 2009. Stably maintained dendritic spines are associated with lifelong memories. Nature 462:920–924.

Yu X, Zuo Y. 2011. Spine plasticity in the motor cortex. Curr Opin Neurobiol. 21:169–174.

Yuan W, Burkhalter A, Nerbonne JM. 2005. Functional role of the fast transient outward K+ current IA in pyramidal neurons in (rat) primary visual cortex. J Neurosci. 25:9185–9194.

Zhang Y, Cudmore RH, Lin DT, Linden DJ, Huganir RL. 2015. Visualization of NMDA receptor-dependent AMPA receptor synaptic plasticity in vivo. Nat Neurosci. 18:402–407.